

## Static structure of glass $\text{Ag}_x(\text{GeSe}_3)_{1-x}$ based on *ab initio* molecular dynamics study

Akihide KOURA<sup>1</sup> and Fuyuki SHIMOJO<sup>1</sup>

<sup>1)</sup> *Department of Physics, Kumamoto University, Kumamoto 860-8555*

(Received May 31, 2017)

We have investigated the static structure of glass  $\text{Ag}_x(\text{GeSe}_3)_{1-x}$  ( $x = 0.15, 0.33,$  and  $0.50$ ) based on *ab initio* molecular dynamics simulations. Even at the lower concentration  $x = 0.15$ , Ag-Ag homopolar covalent bonds sometimes appear and short chain-type fragments are formed. The existence of phase separation may be suggested by the results of Mulliken population analysis and group analysis.

### §1. Introduction

Superionic conducting glass Ag-Ge-Se systems attract many scientists because of their strong probability of high performance solid battery. The experimental measurement of the electric conductivity reported that the high conductivity appears at  $x > 0.3$  when Ag atoms are doped into  $\text{Ag}_x(\text{GeSe}_3)_{1-x}$  composition,<sup>1)</sup> in which Ag ions migrate into the glass network consisting of  $\text{GeSe}_4$  tetrahedral units. Furthermore, it is suggested by X-ray and neutron diffraction experiment combined reverse Monte Carlo (RMC) that Ag-Ag chain-type fragments appear at  $x = 0.5$  with increasing Ag concentration  $x$ .<sup>2),3)</sup> Anomalous X-ray scattering and its RMC results on the glass  $\text{Ag}_{0.5}(\text{GeSe}_3)_{0.5}$  show that the first sharp diffraction peak (FSDP) of structure factor at  $k = 1.05 \text{ \AA}^{-1}$  is caused by Ge-Se correlations.<sup>4)</sup> The results also suggest the existence of a phase separation of Ag atoms and Ag homopolar correlation. However, the bonding properties between Ag-Ag atoms and the stable sites of Ag are still unclear.

We investigated the static structure of superionic glass  $\text{Ag}_x(\text{GeSe}_3)_{1-x}$  ( $x = 0.15, 0.33,$  and  $0.50$ ) based on *ab initio* molecular dynamics simulations. Especially we focused on the Ag-Ag homopolar bonds to see whether they are covalent bonding or not. We also discuss the bonding properties between cations (Ag and Ge) and anion (Se) by Mulliken population analysis.

### §2. Numerical details

We have calculated the electronic states using the projector augmented wave (PAW) method within the framework of the density functional theory,<sup>5),6)</sup> in which the generalized gradient approximation was used for the exchange-correlation energy.<sup>7)</sup> The plane wave cutoff energies are 20 and 120 Ry for the pseudo wave functions and the pseudo charge density, respectively. The  $\Gamma$  point was used for Brillouin zone sampling. Projector functions were generated  $4d^{10}5s^15p^0$ ,  $4s^24p^24d^0$ , and  $4s^24p^44d^0$  states for Ag, Ge, and Se, respectively.

The numbers of atoms are 140 (for  $x = 0.15$ , 6Ag+34Ge+102Se, and for  $x = 0.50$ , 28Ag+28Ge+84Se) and 144 (for  $x = 0.33$ , 16Ag+32Ge+96Se). Molecular dynamics simulations employ Nosé-Hoover thermostat technic to control the temperature,<sup>8),9)</sup> the equations of motion were solved via an explicit reversible integrator.<sup>10)</sup> The time step  $\Delta t$  is 2.9 fs.

We obtained 2 or 3 glassy states at each composition. Starting from the liquid state at 1000 K, the temperature is gradually decreased to 300 K with a cooling rate of 100 K / 5000 steps. The physical quantities of our interest were obtained in the isothermal-isobaric ensembles by averaging over more than 20.3 ps after an equilibration of at least 1.45 ps. The number densities  $\rho$  at room temperature at  $x = 0.15$ , 0.33, and 0.50 were obtained as 0.0335, 0.0355, and 0.0367  $\text{\AA}^{-3}$ , respectively.

### §3. Results and discussion

Figure 1 shows the structure factors  $S_X(k)$ , using X-ray form factors, of glass  $\text{Ag}_x(\text{GeSe}_3)_{1-x}$  obtained theoretically (black solid lines) and experimentally (blue squares<sup>3)</sup> and red circles<sup>4)</sup>). Our results are in good agreement with experimental results.<sup>3),4)</sup> The FSDP at around  $k = 1.0 \text{\AA}^{-1}$  suggests the existence of some medium range order, and this FSDP mainly consists of the partial static structure factors  $S_{\text{GeGe}}(k)$  and  $S_{\text{GeSe}}(k)$ . The fact suggests the existence of Ge-Ge homopolar bonds and  $\text{GeSe}_4$  tetrahedral units.

Next we discuss the local structure in the real space, i.e., partial pair correlation functions  $g_{\alpha\beta}(r)$  shown in Fig. 2. Here, we focused on the correlation between cations, Ge-Ge, Ge-Ag, and Ag-Ag. The cation-cation short range correlations often appear in this concentration range. We separate  $g_{\alpha\beta}(r)$  by using a threshold value of bond overlap populations (OVP)  $p_{\alpha\beta}(\bar{O})$  of which detail is discussed later. The threshold value is  $|\bar{O}| = 0.1$ . The results  $g_{\alpha\beta}^{\text{OVP}}(r)$  are also drawn in Fig. 2. The red solid lines, green dotted lines with circles, and blue dashed-dotted lines mean antibonding, covalent bonding, and no bonding, respectively. As a result, it is clearly seen that the peaks of  $g_{\text{GeGe}}(r)$  at 2.5  $\text{\AA}$ , those of  $g_{\text{GeAg}}(r)$  at around 2.5-3.0  $\text{\AA}$ , and the distribution of  $g_{\text{AgAg}}(r)$  between 2.6 and 3.1  $\text{\AA}$  correspond to covalent bondings. Note that in the Ag-poor state ( $x = 0.15$ , here, only 6 Ag atoms) the Ag-Ag homopolar bonds are not so much, but when they appear, they have covalency.

In Fig. 3, OVP  $p_{\alpha\beta}(\bar{O})$  at  $x = 0.15$ , 0.33, and 0.5 are shown by the black solid, red dotted, and green dashed lines, respectively. Top three and bottom three panels correspond to homo- and hetero-correlations, respectively. The negative and positive regions of the horizontal axis show anti- and covalent bondings, respectively. The OVP  $p_{\text{GeGe}}(\bar{O})$  shows that Ge-Ge bondings consist of mainly anti-bondings, however, they have also a few covalent bondings. The profiles of the range  $\bar{O} < 0$  of  $p_{\text{GeGe}}(\bar{O})$  show the tendency of the concentration dependence for Ag atoms, i.e., the number of strong anti-bondings increases with increasing  $x$ . On the other hand, the profile of  $p_{\text{SeSe}}(\bar{O})$  doesn't change much with increasing  $x$ . For Ag-Ag correlation, the weak covalent bondings exist and the number of the covalent bondings increases with increasing  $x$ . Few Ag-Ag anti-bonding appears in this concentration range. Focusing on  $p_{\alpha\beta}(\bar{O})$  of the hetero correlations, they seem not to show much the concentration

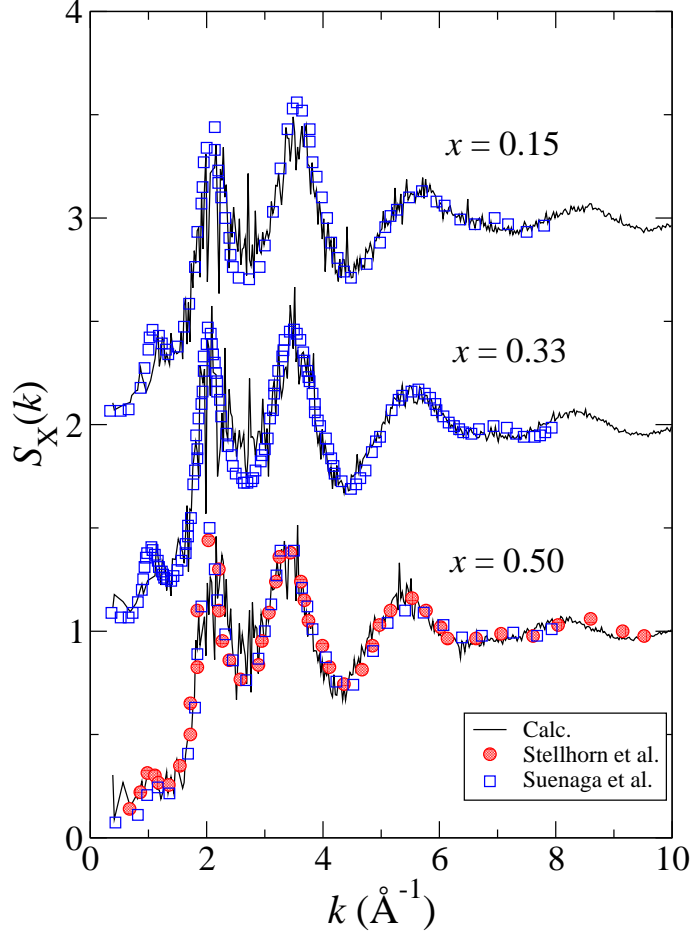


Fig. 1. Structure factors  $S_X(k)$ . Solid lines represent our results. The blue squares and red circles show experimental results by Suenaga<sup>3)</sup> and by Stellhorn,<sup>4)</sup> respectively.

dependence  $x$ . Ag-Ge cation correlation has both anti- and covalent-bondings.

In Fig. 4 shows the concentration dependence of the three body bond angle distribution  $B_{\alpha\beta\gamma}(\theta)$  ( $\alpha, \beta$ , and  $\gamma = \text{Ge, Se, and Ag}$ ). The black solid, red dashed, and green dashed-dotted lines correspond to  $x = 0.15, 0.33$ , and  $0.50$ , respectively. Ge-Se systems at Se-rich region consist of  $\text{GeSe}_4$  tetrahedral units, where Ge and four Se atoms exist at the center and corners of tetrahedral unit, respectively. Therefore the bond angle  $B_{\text{SeGeSe}}(\theta)$  has a peak at approximately  $\theta = 108^\circ$ , and the profile of  $B_{\text{SeGeSe}}(\theta)$  is independent of the Ag concentration  $x$ . The peak positions of  $B_{\text{SeAgSe}}(\theta)$  exist between  $90$  and  $110^\circ$ , and the distributions widely spread. The fact shows that  $\text{AgSe}_4$  tetrahedral units also exist, however the shape of tetrahedral unit is deformed. Figures 4(a) and (b) correspond to the tetrahedral unit-unit angles connected by the corner shared Se atom. The peak position of  $B_{\text{GeSeGe}}(\theta)$  doesn't change with increasing  $x$ . However, its height decreases and the shoulder at approximately  $\theta = 80^\circ$  grows up. On the other hand,  $B_{\text{AgSeAg}}(\theta)$  spreads widely.

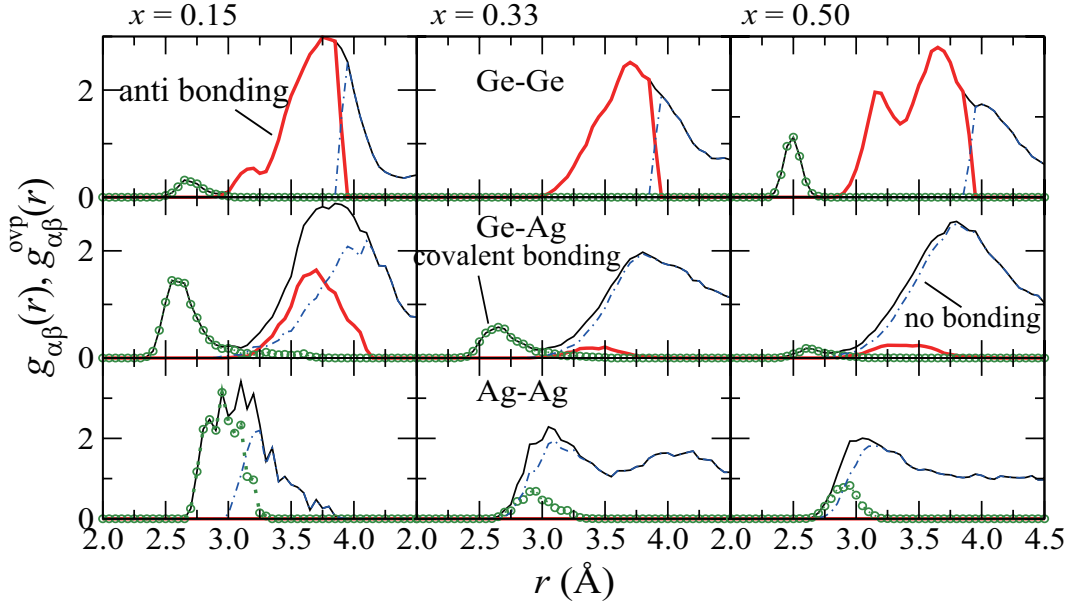


Fig. 2. Partial pair correlation functions  $g_{\alpha\beta}(r)$  drawn by black solid lines for  $\alpha - \beta = \text{Ge} - \text{Ge}$  (top),  $\text{Ge} - \text{Ag}$  (middle), and  $\text{Ag} - \text{Ag}$  (bottom). The red solid lines, the dotted green lines with circles, and the blue dashed-dotted lines indicate antibonding, covalent bonding, and no bonding correlations, respectively.

The bond angle  $B_{\text{GeSeAg}}(\theta)$ , Fig. 4(c), has a peak at almost the same position as the peak position of  $B_{\text{GeSeGe}}(\theta)$  in Fig. 4(a). The profile of  $B_{\text{GeSeAg}}(\theta)$  is similar to  $B_{\text{GeSeGe}}(\theta)$ , however, the distribution is wider. Therefore, although Ge atoms seems to be replaced by Ag atoms, the high diffusivity of Ag atoms makes tetrahedral units to deform.

Next, we estimate the average coordination numbers  $N_{\text{AgAg}}$  using the cutoff distance  $r_c = 3.2 \text{ \AA}$ , which is the minimum of first coordination shell of  $g_{\text{AgAg}}(r)$ . In this first coordination shell of  $g_{\text{AgAg}}(r)$ , Ag-Ag covalent bond clearly exists as shown in Fig. 2.  $N_{\text{AgAg}}$  for  $x = 0.15, 0.33,$  and  $0.50$  are 0.10, 0.47, and 0.74, respectively. For Ge-Ge, using  $r_c = 3.0 \text{ \AA}$ ,  $N_{\text{GeGe}}$  is less than 0.1. For Se-Se, using  $r_c = 2.6 \text{ \AA}$ ,  $N_{\text{SeSe}} = 0.72, 0.63,$  and  $0.46$ , respectively, i.e., Se-chain becomes short with adding Ag atoms. Shortening Se-chain by doping Ag atoms is also suggested by the group analysis for the pair distribution function  $g_{\text{SeSe}}(r)$  (see next paragraph). On the other hand,  $N_{\text{GeSe}}$ , with  $r_c = 3.0 \text{ \AA}$ , keeps around 3.81 in this concentration range. Therefore,  $\text{GeSe}_4$  tetrahedral units are kept in spite of doping Ag atoms.

In Fig. 5, the pair distribution functions  $g_{\text{SeSe}}(r)$  and  $g_{\text{AgAg}}(r)$  of a glass state at each composition are shown. Therefore,  $g_{\text{AgAg}}(r)$  in Fig. 5 are a little bit different from those in Fig. 2. The red dashed lines with circles show  $g_{\alpha\alpha}^{\text{grp}}(r)$ , called the group correlation, calculated from atomic pairs bonded to each other. The green bold lines show  $g_{\alpha\alpha}^{\text{ng}}(r)$ , referred to the non group correlation, calculated from non bonding atomic pairs. Their cutoff distances  $r_c$  of 2.6 and 3.2  $\text{\AA}$  for Se-Se and Ag-Ag pairs,

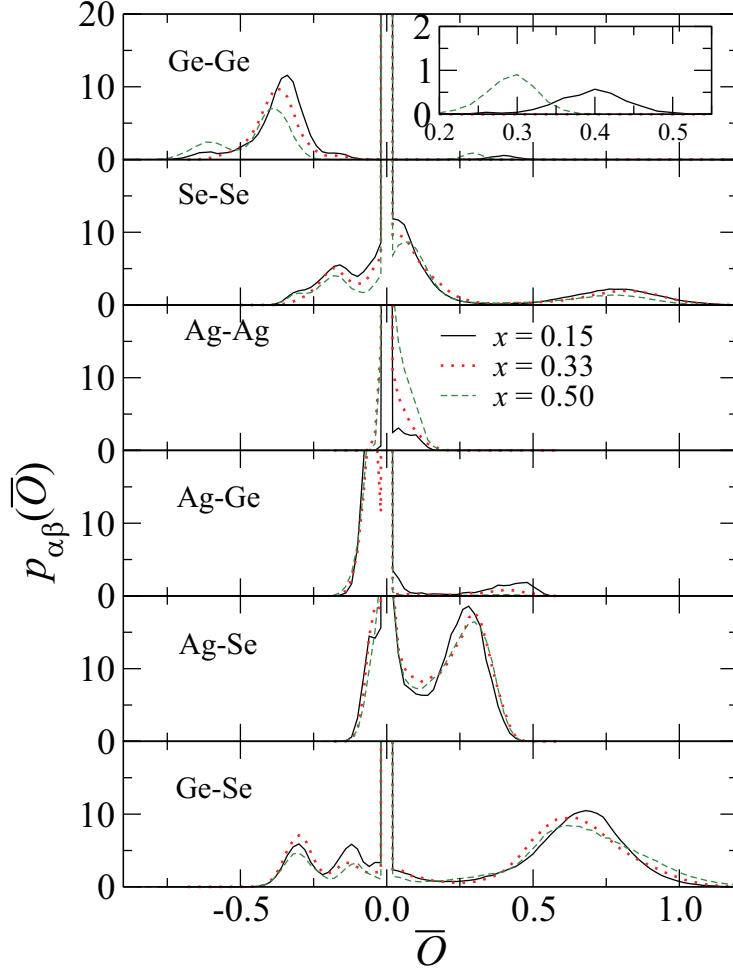


Fig. 3. Concentration dependence of the bond overlap populations  $p_{\alpha\beta}(\bar{O})$ . The black solid, red dotted, and green dashed lines correspond to the Ag concentration  $x = 0.15$ ,  $0.33$ , and  $0.50$ , respectively. The inset of the top panel is focusing on the range  $0.2 < \bar{O} < 0.55$  of  $p_{GeGe}(\bar{O})$ .

respectively, are used to determine whether each atomic pair has covalent bonding or not. At the Ag concentration  $x = 0.15$ ,  $g_{SeSe}^{gfp}(r)$  has two peaks at approximately  $r = 2.4$  and  $3.8$  Å. And, two small humps exist at about  $r = 4.8$  and  $6.8$  Å. These features mean the existence of long Se-chains. With doping Ag atoms, the second peak of  $g_{SeSe}^{gfp}(r)$  at approximately  $r = 3.8$  Å is kept at  $x = 0.5$ , however, the humps at higher  $r$  disappear at  $x = 0.5$ , i.e., Se-chain is shortening with increasing Ag atoms. For Ag-Ag pairs, on the other hand, there is no chain structure at  $x = 0.15$ . At  $x = 0.33$ , small distributions appear at approximately  $r = 3.3$  and  $5.5$  Å. Furthermore, long Ag-Ag group exists at  $x = 0.5$ . The existence of such atom groups may suggest that the phase separation tends to occur.

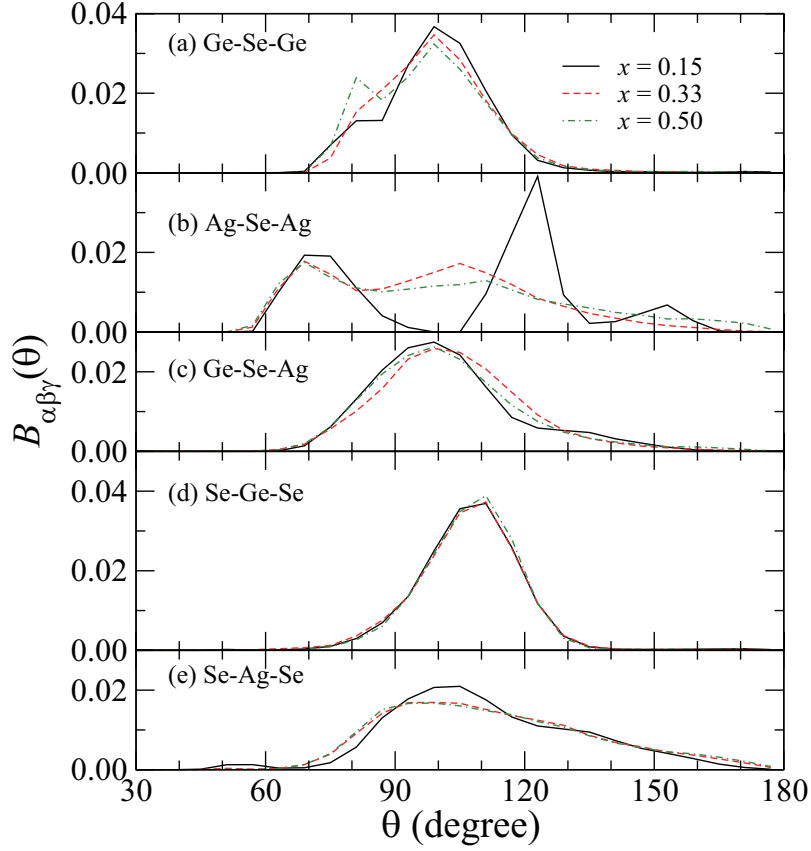


Fig. 4. Concentration dependence of the bond angle distributions  $B_{\alpha\beta\gamma}(\theta)$ . The black solid, red dashed, and green dashed-dotted lines correspond to the Ag concentration  $x = 0.15$ ,  $0.33$ , and  $0.50$ , respectively.

#### §4. Conclusion

We have investigated the structure of superionic conducting glass  $\text{Ag}_x(\text{GeSe}_3)_{1-x}$  ( $x = 0.15, 0.33$ , and  $0.50$ ) based on *ab initio* molecular dynamics simulations. We confirmed the existence of Ag-Ag homopolar covalent bonds. A few Ge-Ge homopolar bonds also appear.  $\text{GeSe}_4$  tetrahedral units exist, and they are connected by not only corner-sharing but also selenium chains. The existence of phase separation is suggested by the results of Mulliken population analysis and the group analysis.

#### Acknowledgements

The authors thank the Supercomputer Center, the Institute for Solid State Physics, University of Tokyo for the use of the facilities. The computation in this work has also been done using the facilities of the Research Institute for Information Technology, Kyushu University.

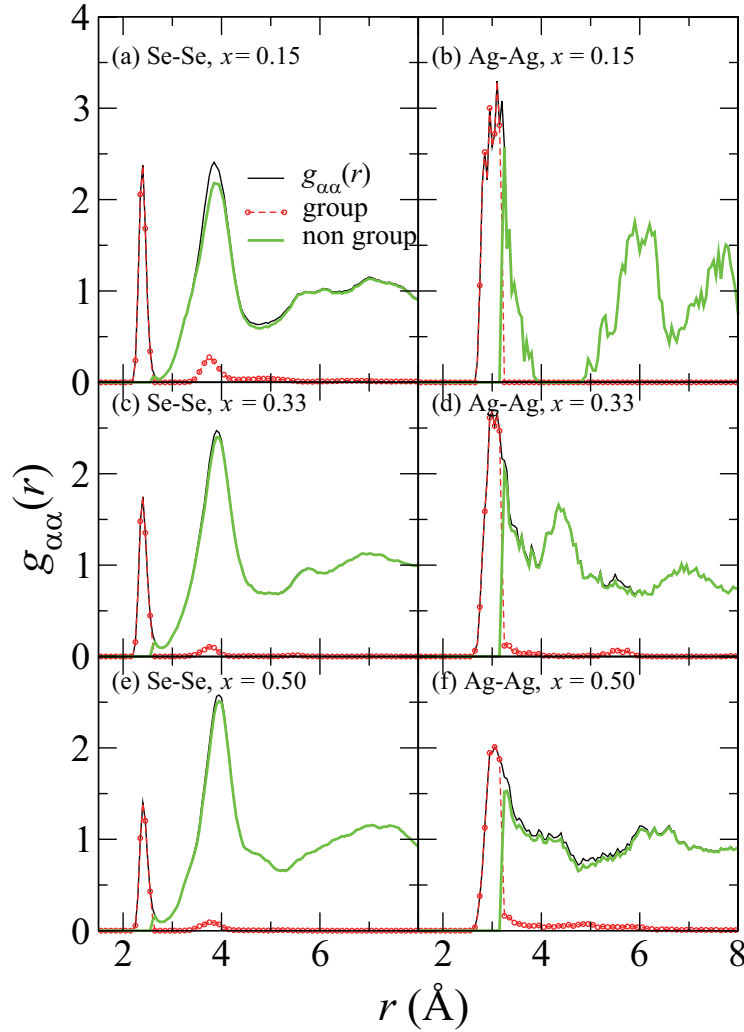


Fig. 5. Concentration dependence of the correlation functions  $g_{\alpha\alpha}(r)$  ( $\alpha = \text{Se}, \text{Ag}$ ). The black solid lines show  $g_{\alpha\alpha}(r)$  of one of the glass state at each concentration. Therefore,  $g_{\text{AgAg}}(r)$  in Fig. 5(b), (d), and (f) are slightly different from those shown in Fig. 2. The red dashed lines with circles show the group correlation function  $g_{\alpha\alpha}^{\text{gp}}(r)$ . The green bold lines show the non group correlation functions  $g_{\alpha\alpha}^{\text{ng}}(r)$ . Details of both correlations  $g_{\alpha\alpha}^{\text{gp}}(r)$  and  $g_{\alpha\alpha}^{\text{ng}}(r)$  are written in the main text.

### References

- 1) M. Kawasaki, J. Kawamura, Y. Nakamura, and M. Aniya: *Solid State Ionics* **123** (1999) 259 .
- 2) K. Ohara, L. S. R. Kumara, Y. Kawakita, S. Kohara, M. Hidaka, and S. Takeda: *J. Phys. Soc. Jpn.* **79** (2010) 141.
- 3) R. Suenaga, Y. Kawakita, S. Nakashima, S. Tahara, S. Kohara, and S. Takeda: *J. Phys. Conf. Ser.* **98** (2008) 012021.
- 4) J. R. Stellhorn, S. Hosokawa, Y. Kawakita, D. Gies, W.-C. Pilgrim, K. Hayashi, K. Ohoyama, N. Blanc, and N. Boudet: *J. Non-Cryst. Solids* **431** (2016) 68 .

- 5) P. E. Blöchl: Phys. Rev. B **50** (1994) 17953.
- 6) G. Kresse and D. Joubert: Phys. Rev. B **59** (1999) 1758.
- 7) J. P. Perdew, K. Burke, and M. Ernzerhof: Phys. Rev. Lett. **77** (1996) 3865.
- 8) S. Nosé: Molecular Physics **52** (1984) 255.
- 9) W. G. Hoover: Phys. Rev. A **31** (1985) 1695.
- 10) M. Tuckerman, B. J. Berne, and G. J. Martyna: J. Chem. Phys **97** (1992) 1990.